Water-mediated conformational transitions in nicotinic receptor M2 helix bundles: a molecular dynamics study

R. Sankararamakrishnan**, M.S.P. Sansom*

Laboratory of Molecular Biophysics, The Rex Richards Building, University of Oxford, South Parks Road, Oxford OX1 3QU, UK

Received 25 September 1995; revised version received 10 November 1995

Abstract The ion channel of the nicotinic acetylcholine receptor is a water-filled pore formed by five M2 helix segments, one from each subunit. Molecular dynamics simulations on bundles of five M2α7 helices surrounding a central column of water and with caps of water molecules at either end of the pore have been used to explore the effects of intrapore water on helix packing. Interactions of water molecules with the N-terminal polar sidechains lead to a conformational transition from right- to left-handed supercoils during these simulations. These studies reveal that the pore formed by the bundle of M2 helices is flexible. A structural role is proposed for water molecules in determining the geometry of bundles of isolated pore-forming helices.

Key words: Ion channel; Transmembrane helix; Water dynamics; Sidechain interactions: Helix bundle geometry

1. Introduction

The nicotinic acetylcholine receptor (nAChR) is a postsynaptic, integral membrane protein. It contains a cation-selective water-filled ion channel [1,2] and is the best-characterized member of the superfamily of neurotransmitter-gated ion channels [3]. Photolabeling experiments using open channel blockers [4,5] and site-directed mutagenesis studies [6–8] implicate the transmembrane segment M2 in forming the lining of the channel. Furthermore synthetic peptides corresponding to the M2 sequence form transbilayer α-helices which self-assemble in lipid bilayers to form cation channels whose properties resemble those of the parent channel protein [9]. Electron diffraction studies of the open [10] and closed [11] states of nAChR at 9Å resolution, reveal that five M2 helices, one from each subunit, form an approximately parallel bundle surrounding a central pore [12]. In the open state of nAChR, the pore is shaped by a 'barrel' of α-helices having a pronounced right-handed twist. In the closed state, the M2 helices twisted around each other in a left-handed fashion. Comparison of open and closed states has led to the suggestion that the transition between these two modes of packing may form the structural basis of channel gating [13]. In the absence of atomic resolution structural data for nAChR, the forces stabilizing the open and closed states and the mechanism of pore opening must be elucidated by less direct structural approaches. Recently, we have carried out modelling studies on pentameric helix bundles of chick M2α7 in order to investigate the packing interactions within these bundles [14]. The results of the studies revealed the influence of inter-helix hydrogen bonding on helix bundle geometry.

Unlike bacteriorhodopsin, in which water molecules are believed to play an important role in its function [15–17], the significance of solvent molecules in nAChRs and in channels formed by synthetic M2 peptides has not been fully explored. In the present paper, we have extended our earlier studies by performing molecular dynamics (MD) simulations on M2 helix bundles solvated within and at the two mouths of the pore with TIP3P waters. Helix bundles with both right- and left-handed coiled coils were considered as the starting points for these MD simulations. The effects of solvent-mediated interactions on changes in helix packing during the course of these simulations are analyzed.

2. Materials and methods

2.1. Computational details

Model building, energy minimization and molecular dynamics (MD) simulations were carried out using XPLOR V3.1 [18] with the CHARMm PARAM19 parameter set [19]. Only those hydrogen atoms attached to the polar groups were represented explicitly; apolar groups were represented using extended atoms. The water model employed to solvate the bundles was the TIP3P three-site model [20] with partial charges $q_O = -0.834$ and $q_H = +0.417$, modified as in the PARAM19 parameter set of CHARMm so as to allow the internal flexibility of water molecules. All calculations were performed on DEC 3000 400 computers. Display and examination of bundles were carried out using QUANTA V4.0 (Molecular Simulations) installed on Silicon Graphics R3000 workstations. Diagrams of the structures were drawn using MOLSCRIPT [21].

2.2. Initial structures for MD simulations

Chicken α7 acetylcholine receptors form homopentameric assemblies [22,23]. Simulated annealing via restrained molecular dynamics (SA/MD) was used to generate ensembles of pentameric M2α7 helix bundles. Initial structures for solvation and MD simulations were selected from these ensembles. SA/MD has been used to study single transmembrane (TM) helices [24,25], simple TM helix bundles [26,27] and M2 helix bundles [12,14]. The initial helix bundle models employed in the current MD simulations have been described in a previous paper [14] to which the reader is referred for further details.

The sequence of M2α7 is:

E K I **S** L G I **T** V L L **S** L T V F M L L V A E

1′ 4′ 8′ 12′

The numbers below the sequence correspond to the channel-lining sidechains shown in bold type and define the numbering scheme used throughout the paper, in which the glutamate residue of the cytoplasmic *intermediate* ring [23] of M2α7 is numbered 1′. The N-termini and C-termini were blocked with an acetyl group and an amide group, respectively, in order to mimic the effect of preceding and succeeding peptide bonds.

On the basis of the sensitivity of open channel block by the local anaesthetic derivative QX-222 to mutations in the sequence of M2, it has been proposed that the QX-222 binds midway down the channel

*Corresponding author. Fax: (44) (1865) 51-0454 or 27-5182. E-mail: mark@biop.ox.ac.uk

**Present address:* Department of Physiology and Biophysics, Beckman Institute, University of Illinois at Urbana-Champaign, Urbana, IL 61801, USA.

0014-5793/95/$9.50 © 1995 Federation of European Biochemical Societies. All rights reserved.
SSDI 0014-5793(95)01376-8

formed by the M2 helices [28]. Model building studies on models of M2 helix bundles, differing in their helix tilt angle (see below) and in the exact orientation relative to the centre of the pore of their pore-lining sidechains, have demonstrated that the individual helices have to be tilted by at least 3° away from the pore axis in order for QX-222 to be able to enter the pore from the C-terminal mouth [29,30]. Models in which the M2 helices were *not* tilted away from the pore axis exhibited a large steric barrier to QX-222 entrance into the pore at the C-terminal mouth. The model in which M2 helices were tilted away from the pore axis by 6° *both* allowed QX-222 to bind within the pore *and* enabled large organic cations which have been demonstrated electrophysiologically to permeate the nAChR channel (e.g. trimethylamine; isobutylamine [31]) to pass through the model pore. Our earlier studies on packing interactions of M2 helix bundles revealed the influence of inter-helix interactions (by residues E1′, K2′ and S4′ residues) on the overall bundle geometry [14]. In the present study, two types of models are considered which differ in their angle of tilt: 3° in Type I; and 6° in Type II. In both the models, the polar residues facing the pore (4′, 8′ and 12′) are oriented such that the N-terminal E1′ and K2′ residues of the ith helix participate in inter-helix interaction with S4′ residue of the $i + 1$th helix. For both models the tilted helices retain significant van der Waals interactions with one another.

The geometry of helix packing within SA/MD-generated helix bundles is described by the average crossing angle (Ω; described by Chothia et al. [32]) between adjacent helices. This parameter can be directly related to the handedness of a coiled coil, with a positive value of Ω corresponding to a left-handed coiled coil. Average Ω values for Type I and Type II ensembles are +8.5° (±2.9) and −9.6° (±7.4) respectively. One M2α7 helix bundle was selected from each ensemble for solvation and further MD simulation studies. These two structures were selected so that their crossing angles were close to the average Ω of their respective SA/MD ensembles. Thus $\Omega = +8.4°$ for the selected Type I bundle and $\Omega = -10.1°$ for the selected Type II bundle were used as the starting structures for the MD simulations.

2.3. Solvation and MD simulation

The lumen of and the two mouths of the pore were solvated using pre-equilibrated TIP3P water molecules. Water molecules in close contact (<1 Å) with the peptide atoms were removed. The resultant solvated structures were energy minimized using the conjugate gradient method until the norm of the gradient of total energy was less than 0.01.

The minimized structures were the starting points for MD simulations. The protocol followed for the simulation is essentially same as described in [24]. The systems were heated gradually from 0 to 300 K in steps of 50 K and at each stage of heating 0.5 ps of dynamics was run. Velocities were rescaled every 0.1 ps during heating and every 1 ps during the equilibration period (22 ps). At the end of equilibration, a further 100 ps simulation was performed, with the systems maintained at a constant temperature of 300 K by coupling to a temperature bath. A constant dielectric ($\varepsilon = 1$) was applied with a cut-off of 9.5 Å for non-bonded interactions. A time step of 0.001 ps was used and intermediate structures were saved every 0.1 ps to yield trajectories for subsequent analysis.

Table 1
Target distances of inter-helix restraints

Restraint[1]	Target distance Å	
	Type I	Type II
H_i (Cα: 2–8) to H_{i+1} (Cα: 2–8)	9.5	9.5
H_i (Cα: 9–15) to H_{i+1} (Cα: 9–15)	10.4	11.8
H_i (Cα: 16–22) to H_{i+1} (Cα: 16–22)	11.3	13.9
H_i (Cα: 2–8) to H_{i+2} (Cα: 2–8)	15.2	15.2
H_i (Cα: 9–15) to H_{i+2} (Cα: 9–15)	16.8	19.0
H_i (Cα: 16–22) to H_{i+2} (Cα: 16–22)	18.3	22.5

[a] Interhelix restraints maintain the tilt of the helices relative to the central pore axis [14] whilst allowing some movement of the helices relative to one another. A restraint H_i to H_{i+1} is between neighbouring helices, whereas a restraint H_i to H_{i+2} acts between next nearest neighbours.

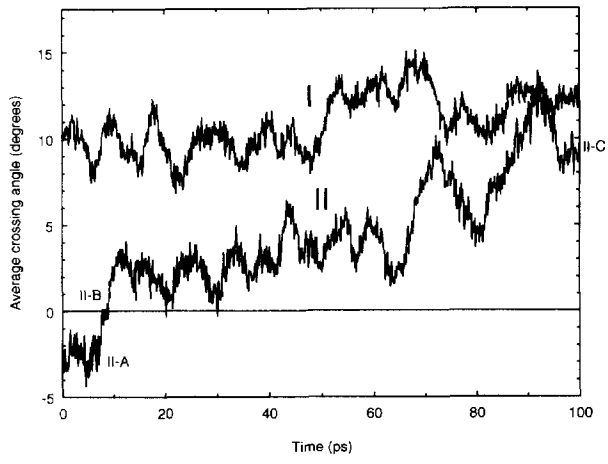

Fig. 1. MD trajectories of the average crossing angle for Type I and Type II M2α7 bundles. The points from which the structures are selected for minimization are indicated along the MD trajectory of Type II bundle.

2.4. Distance restraints

Intra- and inter-helix distance restraints [14,26] were imposed during SA/MD, minimization and MD simulations. Both classes of restraints are implemented using a biharmonic function. Intra-helix restraints were used to maintain an α-helical geometry and so acted between the carbonyl O of residue i and amide H of residue $i + 4$. Inter-helix restraints were employed in order to mimic the effect of surrounding protein and/or lipids within the intact channel protein of peptide helix bundle. They act between pairs of virtual atoms defined as the geometric centres of two groups of Cα atoms. The inter-helix restraints employed for Type I and Type II bundles are defined in Table 1. Note that in Table 1: (a) H_i(Cα:2–8) implies the geometric centre of Cα atoms of residues 2 to 8 of helix i; and (b) the pattern of restraints is cyclic, i.e. for a pentameric helix bundle, H_i to H_{i+1} implies restraints linking helix 1 to 2, 2 to 3, 3 to 4, 4 to 5 *and* 5 to 1. Thus, for Type I bundles the helices are restrained so that the helix axis to z-axis distance is ca. 9.4 Å at the N-terminal mouth and ca. 11.0 Å at the C-terminal mouth; for Type II bundles the corresponding distances are 9.4 Å and 12.5 Å. No restraints were applied to the water molecules.

3. Results

Molecular Dynamics simulations were carried out for both Type I and Type II bundles as described in section 2. At the end of the simulations, there were 1000 MD simulated structures for each of the Type I and Type II models. Bundle geometry, energy components and solvent interactions are analyzed in detail for the MD simulated Type I and Type II structures.

3.1. Geometric and energetic properties

Helix crossing angles were calculated for adjacent pairs of helices and the average Ω was calculated for each bundle. MD trajectories of average crossing angle for both Type I and Type II bundles are shown in Fig. 1. It is striking that while the Type I bundle remained as a left-handed coiled coil (positive Ω) throughout the simulation, the Type II bundle underwent a transition from a right-handed (negative Ω) to left-handed (positive Ω) coiled coil. The Type II bundle remained in a right-handed coiled coil conformation only for a brief period ie about 10 ps at the beginning of the simulation. At $t \approx 10$ ps, a transition occurred. For the next 40 ps or so, the average Ω was below +5°. At $t \approx 65$ ps, the Ω value started increasing further and at the end of the simulation, it stabilized around +9°. In contrast,

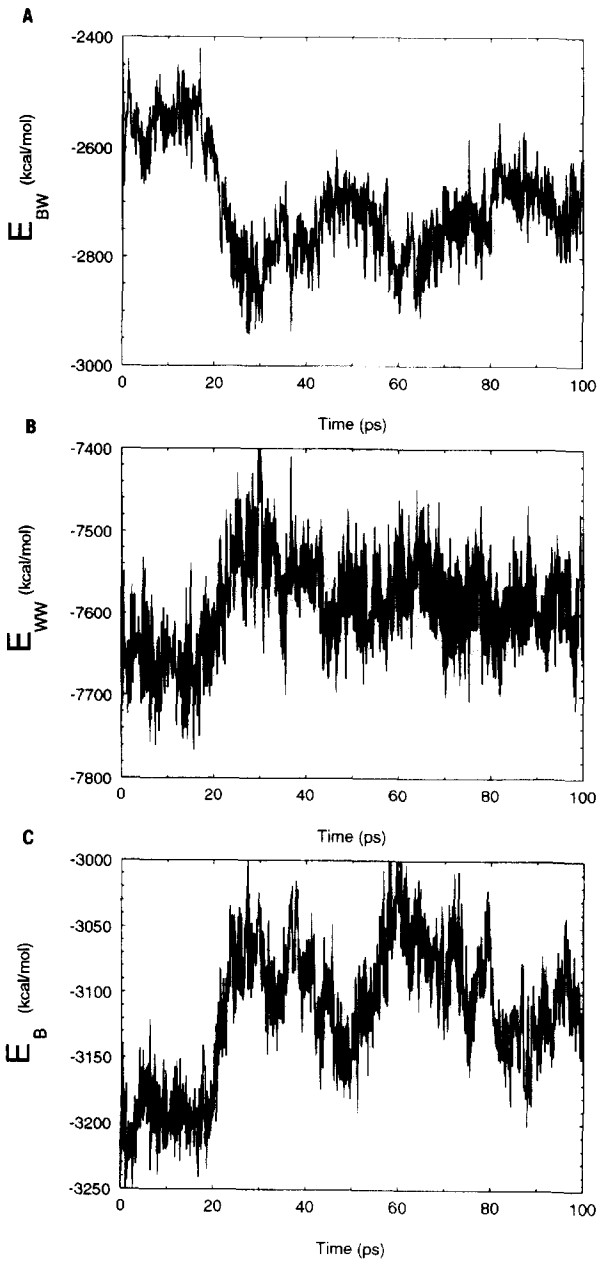

Fig. 2. MD trajectories of energy components due to (A) bundle–water interactions (E_{BW}) (B) water–water interactions (E_{WW}) and (C) the bundle alone (E_B) for the Type II model.

the average Ω was around +10° for the Type I bundle throughout the simulation (Fig. 1).

In order to investigate whether the transition during the MD simulation of Type II bundle is energetically driven, we analyzed various components of energies of the solvated bundles. The total energy (E_{TOT}) of the systems remained approximately constant throughout the simulation for both Type I and Type II bundles. E_{TOT} can be split into the potential energy of the isolated bundle (E_B) and the potential energies of bundle–water interactions (E_{BW}) and of water–water interactions (E_{WW}). Thus $E_{TOT} = E_B + E_{BW} + E_{WW}$. MD trajectories of E_B, E_{BW}, E_{WW} for the Type II model are shown in Fig. 2. It is evident that there is a correlation between these energy components and the transition from right- to left-handed coiled coils in the Type II model (Fig. 1). E_B and E_{WW} increased abruptly after 20 ps and the value of E_{BW} decreased correspondingly coincident with the switch from a right-handed to a left-handed coiled coil. Thus it appears that the switch in handedness results from strengthening of bundle–water interactions. We further analyzed this transition in order to discover which region of the helices contributed to these strengthened interactions with water molecules.

Our previous studies [14] have identified the inter-helix hydrogen bonds formed between sidechains E1′, K2′ of ith helix with S4′ of $i+1$th helix as important factors influencing the geometry of M2α7 helix bundles. The current simulations suggest that the conformational transition from a right-handed to a left-handed coiled coil may result from interaction of water with these sidechains. To establish this we analyzed two energy components: (a) the interaction energy between the N-terminal polar sidechains E1′, K2′ and S4′ (E_{SS}); and (b) interaction energy between these N-terminal sidechains and water molecules (E_{SW}). MD trajectories of E_{SW} and E_{SS} are shown in Fig. 3. There is indeed a direct correlation between the interaction energies of these residues with water molecules and the helix bundle geometry. These results provide clear evidence for a water-driven conformational transition. Interaction energies of water molecules with other channel-lining polar residues T8′ and S12′ did not show any significant variation during the

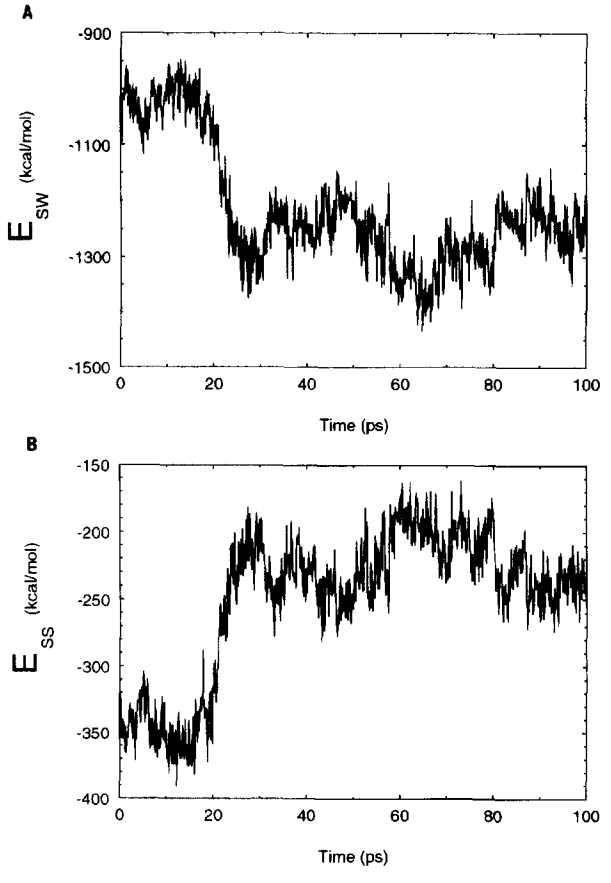

Fig. 3. MD trajectories of energy components due to (A) interactions between water and N-terminal polar (E1′, K2′ and S4′) sidechains (E_{SW}) and (B) interactions between N-terminal sidechains (E_{SS}) for the Type II bundle.

simulation and did not correlate with changes in bundle geometry. These studies therefore suggest that the N-terminal polar residues may play a significant role in determining the helix bundle structure, at least in pores formed by synthetic M2 peptides [2]. However, it should be noted that in the intact nAChR, the other (as yet unidentified) transmembrane segments and a large N-terminal domain may well exert a greater influence in determining the M2 helix bundle geometry.

3.2. Minimization of MD simulated Type II bundles

In order to determine the relative stabilities of right- and left-handed helix bundles, we selected three structures from the Type II MD simulation, namely: structures *II-A* ($\Omega = -4.4°$), *II-B* ($\Omega = +0.8°$) and *II-C* ($\Omega = +9.5°$) corresponding to a left-handed supercoil, no supercoiling and to a right-handed supercoil, respectively. These structures were respectively generated after 4.6 ps, 9.2 ps and 100 ps during the simulation (Fig. 1). These selected structures were energy minimized until the norm of the gradient of the total energy was less than 0.01.

Average crossing angles of these minimized structures remained close to those of their parent structures from the MD trajectory (−3.0° for *II-A*, +0.9° for *II-B* and +9.9° for *II-C*). The radius of the pore through these M2 helix bundles was determined using the program HOLE [33]. The resultant pore radius profiles (Fig. 4) indicate that the changes in the packing within the helix bundles did not significantly alter the overall radius profiles of the pore. The narrowest region of the pore is at the N-termini of the helices, where the radius falls to about 2.5 Å. This constriction is formed by the sidechains of residues E1′, S4′, L5′ and T8′ in all three structures. This radius is such that partial dehydration of Na^+ and K^+ ions would be required in order for them to pass through the pore.

Analysis of energy components shows that the differences in total energies between these three M2α7 helix bundles (*II-A*, *II-B* and *II-C*) are not significant (Table 2). The interaction energy between the water molecules (E_{WW}) dominate the total energy (E_{TOT}) in all the minimized structures. The result that right- and left-handed M2α7 supercoils are energetically equivalent may be true only in helix bundles surrounding an aqueous pore. The minimized structures of *II-A* and *II-C*, representing right- and left-handed coiled coils, are shown in Fig. 5. Again, comparison of various energy components between the minimized structures reveals that the differences are mainly due to

Table 2
Energetics of minimized Type II bundles[a]

Energy components (kcal/mol)	*II-A*	*II-B*	*II-C*
E_{TOT}	−17069	−17085	−17051
E_B	−4014	−4047	−3935
E_{BW}	−2881	−2817	−2926
E_{WW}	−10174	−10221	−10131
E_{SS}	−416	−435	−344
E_{SW}	−1182	−1118	−1292

The energy components are: (a) E_{TOT}, the overall potential energy of the solvated bundle; (b) E_B, the energy of the isolated (i.e. desolvated) bundle; (c) E_{BW}, the bundle/water interaction energy; (d) E_{WW}, the water/water interaction energy; (e) E_{SS}, the interaction energy of the N-terminal polar sidechains (E1′, K2′ and S4′) with one another; and (f) E_{SW}, the interaction energy of the N-terminal polar sidechains with water.

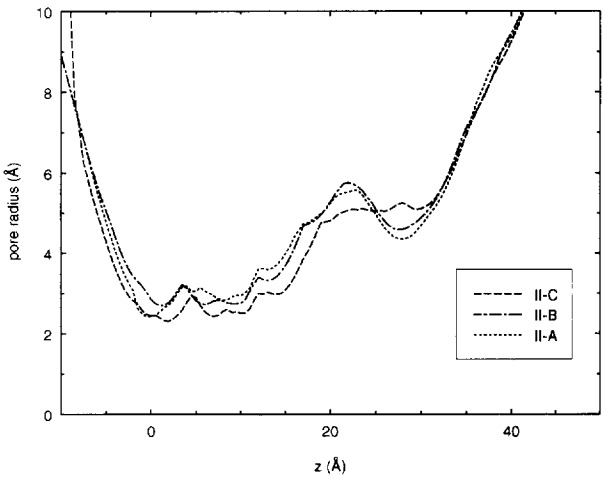

Fig. 4. Pore radius profiles of bundles *II-A*, *II-B* and *II-C*. The N-termini of the helices are at $z \approx 0$ Å and their C-termini are at $z \approx +35$ Å.

different pattern of interactions between water molecules and the N-terminal polar sidechains. The values of energy component E_{SW} reveal that water molecules participate in multiple hydrogen bonds with the N-terminal polar residues, as may be seen in Fig. 5E,F.

4. Discussion

4.1. M2 helix bundle models and ion channels

To what extent do the M2α7 helix bundle models used in the MD simulations described in this paper resemble genuine ion channels? Cryo-electron microscopy studies on open [10] and on closed [11] nAChR show that the M2 helices within the intact protein are kinked near the central leucine (L11′) residue. In contrast, on the basis of the MD simulations described above, and those in previous papers [12,14,24] it appears that isolated M2 helices and helices in isolated M2 bundles do not adopt a kinked conformation. This suggests that in the intact channel interactions of the M2 helix bundle with the surrounding regions of the protein may be the cause of helix kinking. Thus the M2α7 models described in this paper are at best rather approximate representations of helix/helix interactions within the intact channel protein.

Our M2α7 helix bundle models may be somewhat more realistic representations of channels formed by synthetic M2 peptides. Montal and colleagues have synthesized and extensively characterized [9,34] a 23-residue peptide, M2δ, whose sequence is similar to that of M2α7. The M2δ peptide is α-helical and self-assembles in lipid bilayers to form ion channels [9]. Furthermore, template assembled bundles of parallel M2δ helices form ion channels whose properties closely resemble those of the parent nAChR [34–36]. Thus isolated M2 helices are capable of forming bilayer spanning α-helix bundles. Solid-state NMR studies reveal that the helix axis of membrane reconstituted M2δ peptide is parallel to the bilayer normal [37]. In the present studies, the tilt angles of the individual helices relative to the bilayer normal (3° for Type I and 6° for Type II) do not differ significantly from that observed experimentally. Thus the M2α7 structures in the current simulations are plausible models of such simplified ion channels.

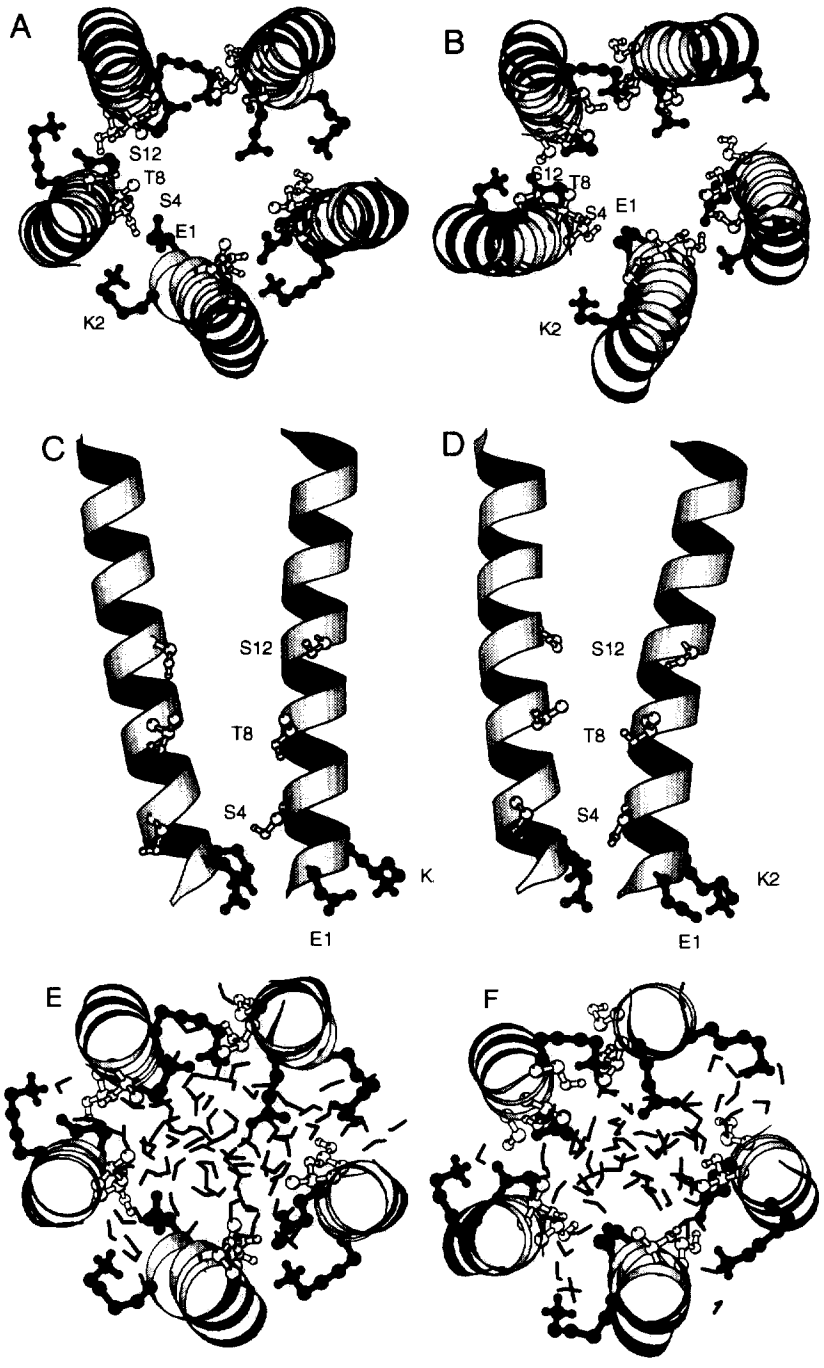

Fig. 5. Structures of bundles *II-A* (A,C,E) and *II-C* (B,D,F) after minimization. In all diagrams, drawn using Molscript [21], the helices are shown as ribbons, the E1′ sidechains are in mid-grey, the K2′ sidechains are in dark grey, and the S4′, T8′ and S12′ sidechains are in white. (A,B) A view down the pore (z) axis, with the C-termini of the helices towards the viewer. (C,D) A view of two adjacent helices of the bundle, perpendicular to z, looking from the centre of the pore outwards. (E,F) A closeup of the region from residue 1′ to residue 8′. The water molecules in this region of the pore are shown in 'bonds only' format.

4.2. Influence of water on helix bundle geometry

Possible roles for water molecules in ion transport [38,39] have been studied in simulations of gramicidin A ion channels. The current studies suggest a structural role for intrapore water molecules in modulating the geometry of packing of pore-forming helices. Water-mediated structural transitions were observed only for Type II bundles. This is thought to be because the weaker van der Waals interactions between the helices (tilted by 6°) facilitated the water-mediated conformational transition. In the Type I model, when the lower tilt angle (3°) results in stronger van der Waals interactions, left-handed coiled coil is maintained throughout the simulation.

Analysis of water dynamics in pores formed by hydrophobic helices, amphipathic peptides and M2α7 helix bundles, shows that water molecules at the mouths of the pore show greater mobility than those inside the pore [40]. Water molecules in-

volved in the interactions with the polar sidechains are near the N-terminal mouth of the pore. The greater mobility of solvent molecules in this region may facilitate the breaking and reforming of sidechain–sidechain and water–sidechain interactions in the N-terminal mouth. Hence conformational transitions additional to those described are possible. This is supported by the minimization results which showed that both left-and right-handed supercoils of M2 helix bundles are of approximately equivalent energy. Overall our simulation studies have demonstrated that a wider hydrophobic C-terminal mouth and the interactions of water molecules with the polar residues in the N-terminal mouth *together* contribute an ion channel with considerable flexibility of helix packing. Such flexibility may underlie the heterogenous conductance levels and life-times observed in channels formed by M2δ peptide helices [9]. In particular, fluctuations in helix packing and in helix/water interactions are expected to modify the electrostatic and steric environment in the N-terminal mouth of the pore and hence the conductance properties of the corresponding channels. However, it is less likely that such flexibility will be present in the intact nAChR protein, which does not exhibit the conductance heterogeneity observed with the isolated peptides. Interestingly, covalent 'tethering' of the C-termini of synthetic M2 helices also results in a reduction of conductance heterogeneity [35].

As discussed above, the M2 bundles considered in this study are approximate models of the pores formed by the M2 synthetic helices and helix bundles in lipid bilayers. We are currently endeavouring to extend this approach to analyze possible roles of water molecules in mediating the transitions between the open and closed states of the intact channel, using models of the latter based upon low-resolution structural data [12].

Acknowledgements: This work was supported by a grant from the Wellcome Trust. Our thanks to Oxford Centre for Molecular Sciences for access to computational facilities and to our colleagues Dr. Ian Kerr and Mr. Jason Breed for discussions.

References

[1] Stroud,R.M., McCarthy, M.P. and Shuster, M. (1990) Biochemistry 29, 11009–11023.
[2] Montal, M. (1995) Annu. Rev. Biophys. Biomol. Struct. 24, 31–57.
[3] Galzi, J.L. and Changeux, J.P. (1994) Curr. Opin. Struct. Biol. 4, 554–565.
[4] Giraudat Dennis, J., Heidmann, M.T., Haumont, P.Y., Lederer, F. and and Changeux, J.P. (1987) Biochemistry 26, 2410–2418.
[5] Hucho, F., Oberthür, W. and Lottspeich, F. (1986) FEBS Lett. 205, 137–142.
[6] Imoto, K., Busch, C., Sakmann, B., Mishina, M., Konno, T., Nakai, J., Buyo, H., Mori, Y., Kukuda, K. and Numa, S. (1988) Nature 335, 645–648.
[7] Leonard, R.J., Labarca, C.G., Charnet, P., Davidson, N. and Lester, H.A. (1988) Science 242, 1578–1581.
[8] Charnet, P., Labarca, C., Leonard, R.J., Vogelaar, N.J., Czyzyk, L., Gouin, A., Davidson, N. and Lester, H.A. (1990) Neuron 2, 87–95.
[9] Oiki, S., Danho, W., Madison, V. and Montal, M. (1988) Proc. Natl. Acad. Sci. USA 85, 8703–8707.
[10] Unwin, N. (1995) Nature 373, 37–43.
[11] Unwin, N. (1993) J. Mol. Biol. 229, 1101–1124.
[12] Sansom, M.S.P., Sankararamakrishnan, R. and Kerr, I.D. (1995) Nature Struct. Biol. 2, 624–631.
[13] Sansom, M.S.P. (1995) Curr. Biol. 5, 373–375.
[14] Sankararamakrishnan, R. and Sansom, M.S.P. (1995) Biochim. Biophys. Acta (in press).
[15] Kandori, H., Yamazaki, Y., Sasaki, J., Needleman, R., Lanyi, J.K. and Maeda, A. (1995) J. Am. Chem. Soc. 117, 2118–2119.
[16] Nina, M., Roux, B. and Smith, J.C. (1994) Biophys. J. 68, 25–39.
[17] Fischer, W.B., Sonar, S., Marti, T., Khorana, H.G. and Rothschild, K.J. (1994) Biochemistry 33, 12757–12762.
[18] Brünger, A.T. (1992) XPLOR Version 3.1: A System for X-Ray Crystallography and NMR, Yale University Press, CT).
[19] Brooks, B.R., Bruccoleri, R.E., Olafson, B.D., States, D.J. Swaminathan, S. and Karplus, M. (1983) J. Comp. Chem. 4, 187–217.
[20] Jorgensen, W.L. (1981) J. Am. Chem. Soc. 103, 335–340.
[21] Kraulis, P.J. (1991) J. Appl. Crystallogr. 24, 946–950.
[22] Couturier, S., Bertrand, D., Matter, J.-M., Hernandez, M.-C., Bertrand, S., Millar, N., Valera, S., Barkas, T. and Ballivet, M. (1990) Neuron 5, 847–856.
[23] Bertrand, D., Devillers-Thiéry, A., Revah, F., Galzi, J., Hussy, N., Mulle, C., Bertrand, S., Ballivet, M. and Changeux, J. (1992) Proc. Natl. Acad. Sci. USA 89, 1261–1265.
[24] Sankararamakrishnan, R. and Sansom, M.S.P. (1994) Biopolymers 34, 1647–1657.
[25] Sankararamakrishnan, R. and Sansom, M.S.P. (1995) Biophys. Chem. 55, 215–230.
[26] Kerr, I.D., Sankararamakrishnan, R., Smart, O.S. and Sansom, M.S.P. (1994) Biophys. J. 67, 1501–1515.
[27] Sansom, M.S.P., Son, H.S., Sankararamakrishnan, R., Kerr, I.D. and Breed, J. (1995) Biophys. J. 68, 1295–1310.
[28] Lester, H. (1992) Annu. Rev. Biophys. Biomol. Struct. 21, 267–292.
[29] Sankararamakrishnan, R. and Sansom, M.S.P. (1995) in: Membrane Protein Models: Experiment, Theory and Speculation (Findlay, J. ed.) chap. 4 (in press), Bios Scientific Publishers, Oxford.
[30] Sankararamakrishnan, R. and Sansom, M.S.P. (1995) Biophys. J. 68, A378.
[31] Dwyer, T.M., Adams, D.J. and Hille, B. (1980) J. Gen. Physiol. 75, 469–492.
[32] Chothia, C., Levitt, M. and Richardson, D. (1981) J. Mol. Biol. 145, 215–250.
[33] Smart, O.S., Goodfellow, J.M. and Wallace, B.A. (1993) Biophys. J. 65, 2455–2460.
[34] Montal Montal, M.S. and Tomich, J.M. (1990) Proc. Natl. Acad. Sci. USA 87, 6929–6933.
[35] Oblatt-Montal, M.O., Iwamoto, T., Tomich, J.M. and Montal, M. (1993) FEBS Lett. 320, 261–266.
[36] Montal, M.O., Iwamoto, T., Tomich, J.M. and Montal, M. (1993) FEBS Lett. 320, 261–266.
[37] Bechinger, B., Kim, Y., Chirlian, L.E., Gesell, J., Neumann, J.M., Montal, M., Tomich, J., Zasloff, M. and Opella, S.J. (1991) J. Biomol. NMR 1, 167–173.
[38] Chiu, S.W., Novotny, J.A. and Jakobsson, E. (1993) Biophys. J. 64, 98–109.
[39] Roux, B. and Karplus, M. (1994) Annu. Rev. Biophys. Biomol. Struct. 23, 731–761.
[40] Breed, J., Sankararamakrishnan, R., Kerr, I.D. and Sansom, M.S.P. (1995) Biophys. J. (submitted).